AIAA 94-0348

Three-Dimensional Coolant Passage Design for Specified Temperatures and Heat Fluxes

G. S. Dulikravich and T. J. Martin
The Pennsylvania State University
University Park, PA

32nd Aerospace Sciences Meeting & Exhibit
January 10-13, 1994 / Reno, NV

THREE-DIMENSIONAL COOLANT PASSAGE DESIGN FOR SPECIFIED TEMPERATURES AND HEAT FLUXES

George S. Dulikravich[1] and Thomas J. Martin[2]
Department of Aerospace Engineering, 233 Hammond Building
The Pennsylvania State University, University Park, PA 16802, USA

Abstract

This paper presents results of research involving the inverse thermal design of coolant flow passage shapes in arbitrary, three-dimensional, internally-cooled configurations. A computer program has been developed to demonstrate this methodology in which a thermal systems designer can simultaneously enforce the desired temperature and heat flux distribution on the hot outer surface of the object while enforcing either the desired temperature, desired heat flux or desired convective heat transfer boundary conditions on the cooled interior surfaces of the coolant flow passages. The program's objective is to meet the over-specified thermal boundary conditions of the outer surface by iteratively altering the geometries of the coolant passages. This is achieved with an automatic, constrained optimization algorithm that minimizes the difference between the user-specified and the intermittently computed hot outer surface heat flux distribution. A quasi-Newtonian gradient search algorithm was used for the optimization. A simple method for escaping stationary points was employed and involved the switching of the objective function when the optimization process stalled at a local minimum. The analysis of the steady-state, non-linear heat conduction within the solid was done using the Boundary Element Method (BEM)[1].

[1] Associate Professor. Associate Fellow AIAA.

[2] Graduate Research Assistant. Student Member AIAA.

I. Introduction

The design of turbines within turbojet and turbofan engines introduces a unique set of requirements for high performance, endurance, light weight and compact size. To meet these requirements, turbines must operate at elevated temperature and pressure levels and must use air as a coolant to be capable of withstanding large numbers of thermal cycles, high heat flux levels and high thermal strain levels. An engineer who might wish to reduce the high thermal plastic strains that cause cracks to form in the coolant passage walls of a turbine blade must simultaneously try to maximize the heat transfer out of the blade to avoid melting. This complicated thermal design problem could be accomplished by allowing the engineer to develop a coolant system geometry that satisfies a specific desired temperature field within the configuration.

The design of internal coolant flow passages within turbine blades is usually accomplished using approximate empirical methods, repetitive numerical analysis of intuitively modified coolant flow passage shapes and expensive experimentation. The development of high speed computers and adequate numerical techniques has made it possible to approach the design problem differently and to solve it more efficiently and with greater accuracy. During the past several years, we have developed a fully automatic inverse thermal design method[2-9] that allows a thermal cooling systems designer to determine the proper sizes, shapes and locations of arbitrary coolant fluid passages within internally cooled configurations. The methodology has been successfully demonstrated on several simple geometries and also on realistic shapes such as coated and non-coated, two- and three-dimensional turbine blades, scramjet combustor struts and rocket nozzle wall sections.

II. Theory

The mathematical model for steady-state heat conduction within an internally cooled solid object can be represented by a boundary value problem over a multiply-connected domain. The desired temperature field within a fixed configuration is intrinsically related to a single set of well-posed thermal boundary conditions specified on the object's surface. If additional boundary conditions are enforced on part or all of the object's surface, the boundary value problem becomes ill-posed but not necessarily multi-valued. The methodology presented in this paper demonstrates that this problem may be solved by iteratively altering the geometry of the configuration until the over-specified thermal boundary conditions are appropriately satisfied.

Steady-state heat conduction in a nonhomogeneous, isotropic medium with a variable coefficient of thermal conductivity is governed by the following partial differential equation in the region, Ω, of a conducting solid

$$\nabla \bullet \left(\lambda(T) \nabla T \right) = 0 \qquad (1)$$

where T is the temperature and $\lambda(T)$ is the temperature-dependent coefficient of thermal conductivity. This equation represents a boundary value problem having essential boundary conditions, T_0, and natural boundary conditions, Q_0, specified on the surfaces Γ_u and Γ_q, respectively. Equation (1) can be linearized by the application of the classical Kirchoff transformation[10] which defines the heat function, Θ, as

$$\Theta = \int_0^T \frac{\lambda(T)}{\lambda_o} \, dT \qquad (2)$$

Here, λ_o is a reference conductivity. Utilizing this transformation, equation (1) can be transformed into Laplace's equation and solved for the heat function, Θ, instead of the temperature, T.

$$\nabla^2 \Theta = 0 \qquad (3)$$

Results obtained for the heat function must be transformed back into temperatures using the inverse of the transformation given in equation (2).

The Laplace's equation can be accurately and efficiently solved using the BEM[1]. By introducing an approximation, u, to the exact solution, Θ, an error function or residual is produced in the domain and on the boundary. The residual in the domain is given by $R = \nabla^2 u$ and the residuals in the essential and natural boundary conditions are

$$R_u = u - \Theta_0 \quad \text{and} \quad R_q = \partial u/\partial n - Q_0 \qquad (4)$$

respectively. These error functions are normally non-zero unless u is the exact solution. The weighted average of the residual over the domain and on the boundary may be set to zero by the weighted residual statement

$$\int_\Omega u^* \nabla^2 u \, d\Omega - \int_{\Gamma_q} (q - Q_0) u^* \, d\Gamma + \int_{\Gamma_u} (u - \Theta_0) q^* \, d\Gamma = 0 \qquad (5)$$

where u* represents the weight function which is usually called the fundamental solution[1], while $q = \partial u/\partial n$ and $q^* = \partial u^*/\partial n$ where **n** is the direction of the outward normal to the surface Γ. After integrating by parts twice, the boundary integral equation for Laplace's equation is obtained

$$\int_\Omega u \nabla^2 u^* \, d\Omega + \int_\Gamma u^* q \, d\Gamma = \int_\Gamma q^* u \, d\Gamma \qquad (6)$$

The weight function is a Green's function solution for a point-source subject to the homogeneous boundary conditions. For the three-dimensional Laplace's equation it is

$$u^* = \frac{1}{4\pi r} \qquad (7)$$

where $r = | \mathbf{x}_i - \mathbf{x}_j |$, $\mathbf{x}_i$ is the coordinate of the observation point and $\mathbf{x}_j$ is the coordinate of the source point. The bounding surface Γ is discretized into N_{SP} surface elements bounded by N end-nodes. After discretizing the surface and utilizing the properties of the Dirac delta function, the boundary integral equation (6) can be written as

$$c_i u_i + \sum_{j=1}^{Nsp} \int_{\Gamma_j} u \, q^* \, d\Gamma_j = \sum_{j=1}^{Nsp} \int_{\Gamma_j} q \, u^* \, d\Gamma_j \qquad (8)$$

for each "i-th" node. The term c_i indicates the scaled internal angle at the i-th surface node. It is produced

when the first surface integral of equation (6) is integrated in the sense of the Cauchy principal value. The functions u and q are assumed to vary bilinearly along each quadrilateral surface element and, therefore, they can be defined in terms of their nodal values and interpolation functions. The whole set of equations for the N nodal values of u and q can be expressed in matrix form as

$$[\mathbf{H}]\,\mathbf{U} = [\mathbf{G}]\,\mathbf{Q} \tag{9}$$

where $\mathbf{U} = (U_1, U_2, \ldots, U_N)$ and $\mathbf{Q} = (Q_1, Q_2, \ldots, Q_{Nsp})$ are vectors containing the nodal potentials and surface panel fluxes respectively while the terms in the [**H**] and [**G**] matrices are assembled by properly adding the contributions from each surface integral.

After the [**H**] and [**G**] matrices are formed, all boundary conditions are applied and a set of linear algebraic equations, $[\mathbf{A}]\,\mathbf{X} = \mathbf{F}$, is constructed. Known or specified surface potentials, U_j, and fluxes, Q_j, are assembled on the right-hand-side of the equation set and are multiplied by their respective [**H**] or [**G**] matrix row thus forming the vector of knowns, **F**. All unknown potentials or fluxes are assembled on the left-hand-side of the equation set and are represented by a coefficient matrix [**A**] multiplying a vector of unknown quantities, **X**.

The integration for each surface panel in equation (8) was performed with three-point Gaussian quadrature. Whenever the surface panel integral included a singularity at one of the quadrilateral's vertices, a localized transformation[11] was performed to eliminate the singularity and the order of the Gaussian quadrature was increased to a five-point integration.

III. The Optimization Technique

The complexity of the analysis of the temperature field in an irregular, three-dimensional, multiply-connected domain calls for the use of a relatively simple but robust and fast optimization technique for constrained, nonlinear optimization. The Davidon-Fletcher-Powell (DFP) quasi-Newton algorithm[12-13] was implemented because it requires a relatively low number of objective function evaluations and because of its ability to converge quickly near minima. This optimization procedure is iterative in nature and involves repetitive solutions of the thermal field within the solid configuration. A first-order numerical approximation was used to compute the gradients of the objective function and the univariant line search was handled using quadratic polynomial fitting.

The primary goal of the optimization procedure is the minimization of the objective function $f(\mathbf{x})$, where **x** contains the N_{VAR} design variables which make up the geometry of the internal coolant passages. During the optimization process local minima can occur and halt the process before achieving an optimal solution. In order to overcome such a situation, a simple technique has been devised[14]. In this approach, whenever the optimization stalls, the formulation of the objective function is automatically switched to some other valid formulation. The new objective function provides a departure from the local minima and further convergence towards the global minimum.

Specifically, the objective of the optimization procedure is to minimize the difference between the specified heat fluxes, Q^{spec}, and the calculated values, Q^{calc}, at the outer boundary. Thus, the objective function can be mathematically formulated in the sense of the normalized least squares of the global error

$$f(\mathbf{x}) = \frac{\sum_{j=1}^{N} (Q_j^{spec} - Q_j^{calc})^2}{\sum_{j=1}^{N} (Q_j^{spec})^2 + \varepsilon} \tag{10}$$

or as a local normalized error at each panel on the outer boundary.

$$f(\mathbf{x}) = \sum_{j=1}^{N} \frac{(Q^{spec} - Q^{calc})^2_j}{(Q^{spec})^2_j + \varepsilon} \tag{11}$$

Here, ε is a very small user-specified parameter to avoid division by zero.

In summary, the optimization procedure consists of the following steps:

(1) The geometry of the outer surface of the object is assumed fixed in order to satisfy certain requirements. This configuration may be supplied as a surface grid only due to the nature of the BEM thermal field analysis.

(2) The desired temperature and heat flux profile are specified on the hot outer surface of the turbine blade. The temperature is used as a Dirichlet-type

boundary condition on the outer surface while the heat flux profile is used in the objective function formulation of the optimization procedure described previously. In addition, boundary conditions such as temperature, heat flux or the convective heat transfer function must be specified on the three-dimensional coolant passage surfaces. The configurations of which are, as yet, unknown.

(3) The user may specify almost any type of equality or inequality constraints to the program as a subroutine. Such constraints could be allowable minimum or maximum wall thickness, minimum distance between multiple coolant passage walls, minimum or maximum cross-sectional areas of the coolant channels, material types and properties, etc. The program is already capable of handling infeasible geometries as additional constraints.

(4) The user supplies an initial guess geometry for the internal configuration. This is given as a set of design variables that makes up the geometry of the three-dimensional coolant flow passages.

(5) The BEM is used to solve for the temperature field within the current configuration. Since the temperature boundary conditions are specified on the outer surface, the BEM algorithm automatically computes the heat flux distribution on that surface. The computed heat flux distribution is, in general, not the same as the user-specified heat flux distribution.

(6) An objective function is formulated using the computed and user-specified outer surface heat fluxes. Please note that the use of heat fluxes in the objective function is not a requirement nor a limitation. The user is free to develop any objective function or set of weighted objective functions that may utilize not only boundary values such as temperature and heat flux, but also convective heat transfer coefficients and ambient temperatures, temperatures at points within the solid, thermal stresses and strains and many other functions of the temperature field.

(7) The optimization procedure automatically perturbs the design variables in order to minimize the objective function while satisfying the constraints. In order to properly and efficiently minimize this function, a feasible and descent line search direction is found by computing the gradient of the function. This requires one thermal field analysis using the BEM per design variable. Once the line search direction is obtained from the DFP update formula, a univariant sub optimization procedure minimizes the objective function along that direction.

(8) The optimization continues to the next cycle beginning with step 5.

IV. Verification of the Nonlinear Boundary Element Formulation

The accuracy of the BEM analysis program for the nonlinear heat conduction in a 1.0 m long by 0.1 m high by 0.1 m wide parallelepiped object was verified. The rectangular box was discretised with 42 square surface panels each measuring 0.1 m by 0.1 m. Four sides of the object were kept adiabatic ($Q_0 = 0$) and the remaining two opposite planes were subject to different temperatures (T_{hot} = 100 K and T_{cold} = 0 K). The temperature-dependent thermal conductivity was given as a polynomial function

$$\lambda(T) = \lambda_0 (AT^{-1} + B + CT + DT^2 + ET^3) \quad (12)$$

where λ_0 = 1.0 W/ m K, B = 1.0 and A = D = E = 0. Temperature data was collected for various degrees of non-linearity given by one parameter C. The results shown in Figure 1 were compared with the one-dimensional analytic solution[10]

$$\frac{C}{2}T^2 + T = \left(T_{hot} + \frac{C}{2}T_{hot}^2\right) - \left(1 + \frac{C}{2}(T_{hot} + T_{cold})\right)\frac{(z - z_{hot})}{(z_{cold} - z_{hot})}(T_{hot} - T_{cold}) \quad (13)$$

Figure 1 shows that the nonlinear BEM results compared very well with the analytic solution, averaging an error of less than 0.5%.

V. Inverse Design of a Super-elliptic Cavity Within a Sphere.

This test case was used to demonstrate the fully three-dimensional inverse design capability[7] of the optimization algorithm with the BEM thermal field analysis scheme. The geometry consisted of a unit sphere with an off-centered cavity of a three-dimensional super-elliptic shape given by

$$\left(\frac{x - x_0}{a}\right)^n + \left(\frac{y - y_0}{b}\right)^n + \left(\frac{z - z_0}{c}\right)^n = 1 \quad (14)$$

Seven design variables are derived from this equation: the center of the super-elliptic cavity

(x_o,y_o,z_o), its semi-major axes (a,b,c) and the super-elliptic exponent, n. The outer spherical surface and the internal super-elliptical cavity (Fig. 2) were discretized with 64 isoparametric quadrilateral panels, respectively. A temperature of 100 K was specified on the outer surface and 50 K on the inner super-elliptic surface. The normal temperature derivative specified on the outer surface was taken from the analytic solution ($\partial T/\partial n$ = 59.3 K/m) corresponding to the desired (target) configuration consisting of a centered spherical cavity with radius of 0.5 m. The material properties were assumed such that the thermal conductivity λ_o = 1.0 W/m K, A = D = E = 0, B = 1.0, and C = 0.01 K^{-1}.

The initial guess to the design variables was; x_o = 0.2 m, y_o = 0.2 m, z_o = 0.2 m, a = 0.3 m, b = 0.4 m, z = 0.5 m, n = 4.0. The run was terminated near the global minimum with an objective function value of 0.32%. The DFP optimization algorithm nearly reached the fully converged sphere-within-a-sphere configuration (Fig. 3) in 50 optimization cycles. Figure 4 depicts the convergence history of the composite objective function. Note that a spike occurs at the 30th iteration indicating an automatic cost function switch from global to local L2 norm. The entire optimization procedure required 647 calls to the BEM analysis routine and consumed approximately 2235 seconds of CPU time on an IBM 3090 computer.

VI. Inverse Design of a Coolant Passage within a Turbine Blade

This example involved the application of the inverse design technique to a three-dimensional turbine blade of realistic shape. The turbine blade was given a single internal coolant flow passage. The blade inner surface was generated at each radial cross section by first determining the mean thickness curve from the local blade airfoil geometry. At each blade cross section this mean thickness curve was then reduced by a fraction of its total length from the leading and trailing edges, p_{te} and p_{le}, respectively. The local blade airfoil inner contour was then constructed by defining a wall thickness function versus the blade airfoil outer contour arc length, s. The wall thickness was defined to be the distance from a point on blade airfoil outer contour to the corresponding point on the reduced mean thickness curve. The wall thickness t(s) was approximated by a Chebyshev polynomial[15] of degree n given as

$$t(s) \approx \sum_{j=1}^{n} c_j P_{j-1}(s) - \frac{c_1}{2} \qquad (15)$$

where the Chebyshev coefficients are

$$c_j = \frac{2}{n}\sum_{k=1}^{n} t\left[\cos\left(\frac{\pi(k-1/2)}{n}\right)\right]\cos\left(\frac{\pi(j-1)(k-1/2)}{n}\right) \qquad (16)$$

and

$$P_j(s) = \cos(j \arccos s) \qquad (17)$$

The polynomial of equation (15) can be truncated to a lower degree m << n due to the nature of the Chebyshev approximation. Thus, the design variables that made up the coolant passage geometry consisted of m Chebyshev coefficients for each radial section of the blade in addition to the two quantities, p_{te} and p_{le}, that determine by what fraction the mean thickness curve is reduced from the trailing and leading edges of each local blade airfoil.

The outer surface and the initial guess to the inner surface geometry of the three-dimensional turbine blade are shown in Figure 5. The outer surface of the blade was generated by creating airfoil sections of the blade at each of the five locations measured radially from the turbine axis. Each turbine blade section between two consecutive radial cuts was discretised with 20 clustered quadrilateral surface panels around its outer surface in addition to the same number of quadrilateral surface panels on its inner surface. There were also 20 quadrilateral panels covering the blade root cross section and 20 quadrilateral panels covering the blade tip cross section. This means that the blade wall thickness at the root and at the tip sections was discretised by single rows of quadrilateral panels. Consequently, we used a total of 200 quadrilateral surface panels connected between 200 nodes at the panels' vertices.

The desired temperature was prescribed along the outer surface of the turbine blade according to a simple formula

$$T(s) = T_{min} + (T_{max} - T_{min})\left[\cos\left(\frac{2\pi s}{s_{max}}\right)\right]^2 \qquad (18)$$

with T_{min} = 500 K and T_{max} = 1000 K at the blade root section. Each of them was increased by 50 K at each of the four remaining consecutive sections so that their values at the blade tip section were T_{min} = 700 K and T_{max} = 1200 K. The three-dimensional blade surface isotherms are illustrated in Figure 6. In addition, a desired constant temperature was specified on the inner surface, T_{inner} = 300 K. The reference coefficient of thermal conductivity was λ_o = 23.0 W/m K and the parameters of equation (12) were A = D = E = 0, B = -1.0 and C = 0.01 K^{-1}.

Next, a desired (target) configuration for the three-dimensional coolant passage geometry was generated and this is illustrated in Figure 7. The BEM was run once with the desired temperature boundary conditions described above and the outer surface heat fluxes were computed (Fig. 8). These outer surface heat fluxes were then used as the desired (target) over-specified boundary conditions for the optimization process's objective function.

Figures 9a through 9e illustrate the evolution of the coolant passage geometry throughout the optimization process. Each figure represents a consecutive cross-section of the turbine blade showing nodes on the outer surface of the airfoil shape, the initial guess geometry (finely dotted line), several intermittent contours depicting the coolant passage cross-section geometry after every 10 iterations (dashed lines) and the target configuration (solid line). The final configurations are almost geometrically equivalent to the target configurations. The optimization process was completed after 46 iterations with the objective function reducing from an initial value of 74% to its final value of 8.64 % (Figure 10). A single objective function automatic switch occurred at the 14th iteration. Notice also that the objective function declines very rapidly initially and then levels off to a rather slow rate of decrease. This is typical of most optimization procedures. Although the program was terminated at the 46th optimization cycle, the process could be resubmitted in order to further refine the coolant passage geometry. The entire optimization process required 2996 calls to the BEM analysis routine and consumed approximately 2550 seconds of CPU time on a CRAY C-90 single-processor computer.

VII. Summary

The concept of inverse design of three-dimensional configurations subject to over-specified thermal boundary conditions has been found to be feasible. Future research possibilities in the field of three-dimensional shape inverse design using the presented methodology could be directed toward complex design tools involving thermal convection, radiation and conduction as well as thermal stress-deformation field analysis and electromagnetic field problems. The same optimization procedure with boundary integral analysis described herein can be used for problems governed by Poisson's equation. This work is presently being extended into unsteady, fully three-dimensional, nonlinear heat conduction involving latent heat, multiple coolant passages and multiple domains with different properties.

VIII. Acknowledgments

Authors are grateful for the remote access to NASA Ames Research Center NAS facility Cray C-90 computer granted by NASA Lewis Research Center. Post processing was performed on the equipment donated by Apple Computer. Mr. Norman F. Foster's help with the graphics is gratefully acknowledged.

IX. References

1. Brebbia, C.A. and Dominguez, J., Boundary Elements: An Introductory Course, McGraw-Hill Book Company, 1989.

2. Kennon, S.R., and Dulikravich, G.S., "The Inverse Design of Internally Cooled Turbine Blades", *ASME Journal of Engineering for Gas Turbines and Power*, pp. 123-126, January 1985.

3. Kennon, S.R. and Dulikravich, G.S., "Inverse Design of Multi-holed Internally Cooled Turbine Blades", *Internat. J. of Numerical Methods in Engineering*, Vol. 22, pp. 363-375, 1986.

4. Chiang, T.L. and Dulikravich, G.S., "Inverse Design of Composite Turbine Blade Circular Coolant Flow Passages", *ASME J. of Turbomachinery*, Vol. 108, pp. 275-282, 1986.

5. Dulikravich, G.S. and Kosovic, B., "Minimization of the Number of Cooling Holes in Internally Cooled Turbine Blades", *International Journal of Turbo & Jet Engines*, Vol. 9, No. 4, pp. 277-283, 1992.

6. Dulikravich, G.S., "Inverse Design of Proper Number, Shapes, Sizes and Locations of Coolant Flow Passages", *Proceedings of the 10th Annual CFD Workshop*, Editor: R. Williams, NASA MSFC, Huntsville, AL, April 28-30, 1992

7. Dulikravich, G.S. and Martin, T.J., "Determination of Void Shapes, Sizes and Locations Inside an Object with Known Surface Temperatures and Heat Fluxes", *Proceedings of the IUTAM Symposium on Inverse Problems in Engineering Mechanics*, Editors: M. Tanaka and H.D. Bui, Tokyo, Japan, May 11-15, 1992.

8. Dulikravich, G.S. and Martin, T.J., "Determination of the Proper Number, Locations, Sizes and Shapes of Super-elliptic Coolant Flow Passages in Turbine Blades", *Proceedings of the International Symposium on Heat and Mass Transfer in Turbomachinery (ICHMT)*, Editor: R.J. Goldstein, Athens, Greece, Aug. 24-28, 1992.

9. Dulikravich, G.S. and Martin, T.J., "Inverse Design of Super Elliptic Coolant Passages in Coated Turbine Blades with Specified Temperatures and Heat Fluxes", Symposium on Multidisciplinary Analysis and Optimizations (AIAA/ USAF/ NASA/ OAI), *AIAA paper 92-4714*, Cleveland, OH, Sept. 21-23, 1992c; to appear in *AIAA Journal of Thermophysics and Heat Transfer*, Jan.-March.1994.

10. Chapman,A.J., Heat Transfer, McMillan Co., New York, 1960.

11. Telles, J.C.F., "A Self-Adaptive Co-Ordinate Transformation for Efficient Numerical Evaluation of General Boundary Element Integrals", *Int. J. for Numer. Meth. in Eng.*, Vol. 24, pp. 959-973, 1987.

12. Vanderplaats, G.N., Numerical Optimization Techniques for Engineering Design, McGraw-Hill, New York, 1984.

13. Arora, J.S., Introduction to Optimum Design, McGraw-Hill Book Company, 1989.

14. Dulikravich, G.S., "Inverse Design and Active Control Concepts in Strong Unsteady Heat Conduction", *Applied Mechanics Reviews*, Vol. 41, No. 6, June 1988, pp. 270-277.

15. Press, W.H., Teukolsky, S.A., Vetterling, W. T. and Flannery, B.P., Numerical Recipes in FORTRAN: The Art of Scientific Computing, Second Edition, Cambridge University Press, 1992.

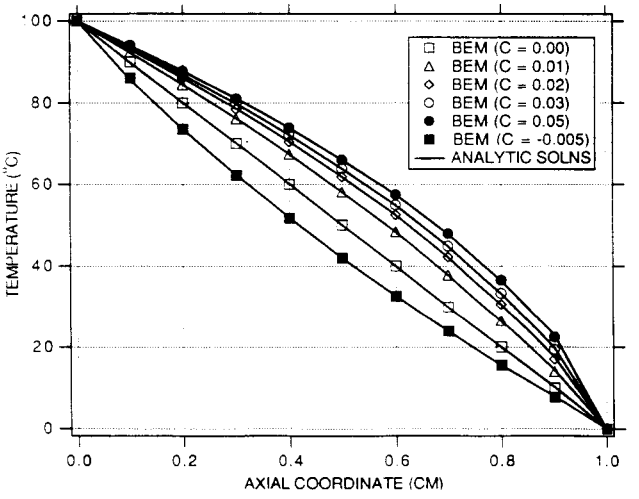

Fig. 1 Comparison of temperature distribution in a parallelepiped with different degrees of thermal dependency of heat conductivity coefficient.

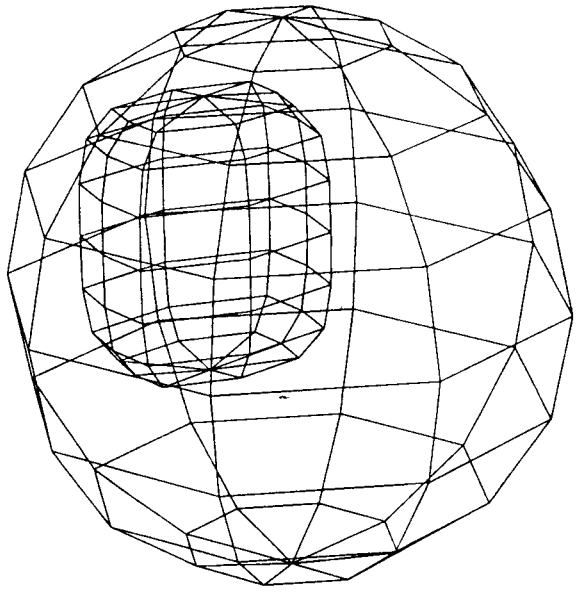

Fig. 2 Initial configuration for a three-dimensional inverse shape design: a super-elliptic off-center cavity in a sphere.

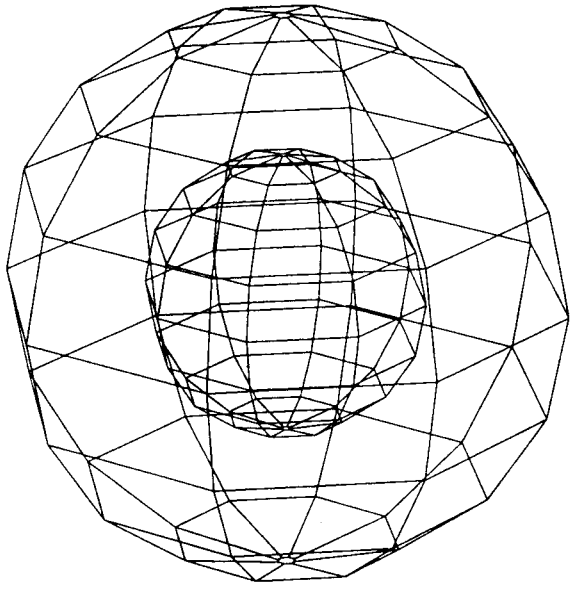

Fig. 3 Final converged configuration for a three-dimensional inverse shape design: a centered spherical cavity in a sphere.

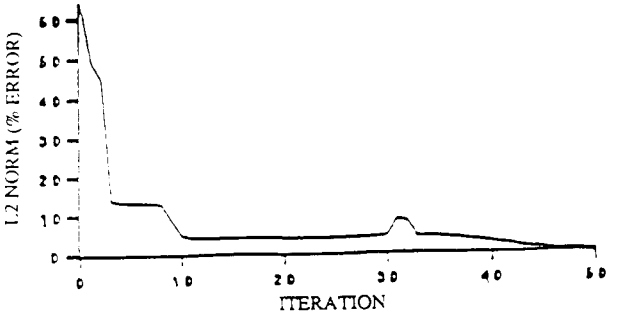

Fig. 4 Convergence history of the objective function for the cavity-in-the-sphere design.

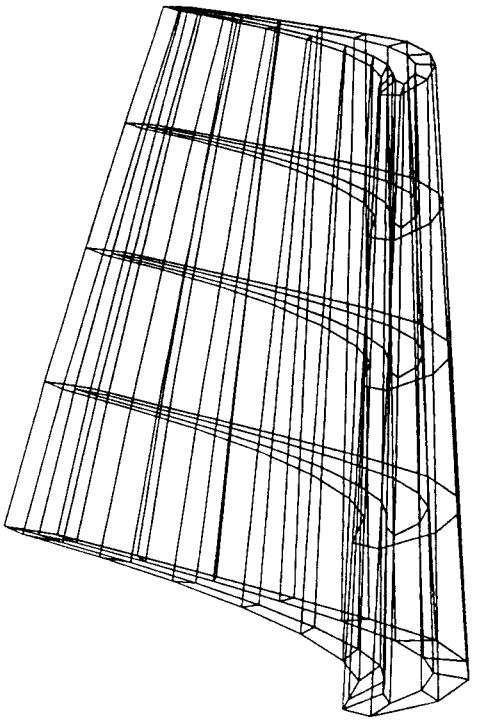

Fig. 5 Initial configuration for a three-dimensional turbine blade with surface discretization.

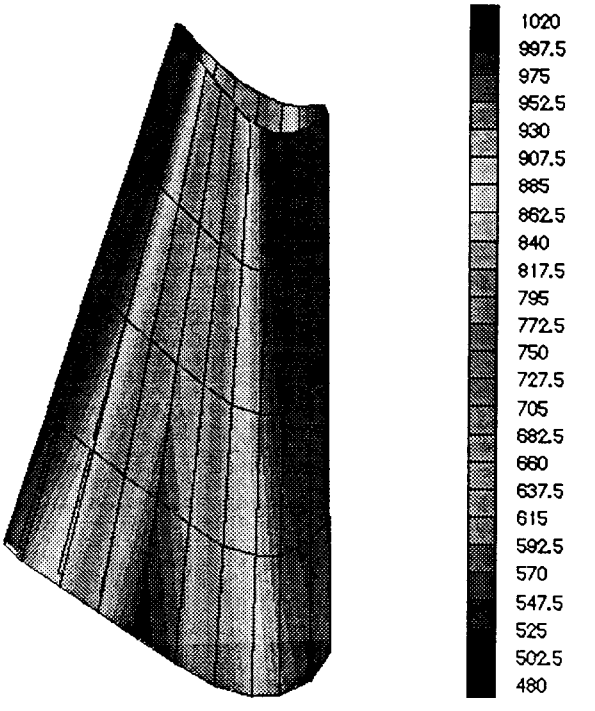

Fig. 6 Specified distribution of temperature on the outer surface of the three-dimensional blade.

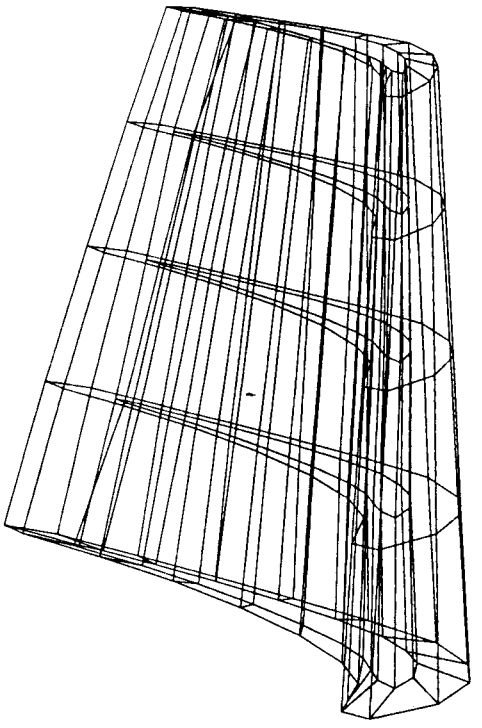

Fig. 7 Specified (desired or target) configuration of the coolant passage inside the three-dimensional turbine blade.

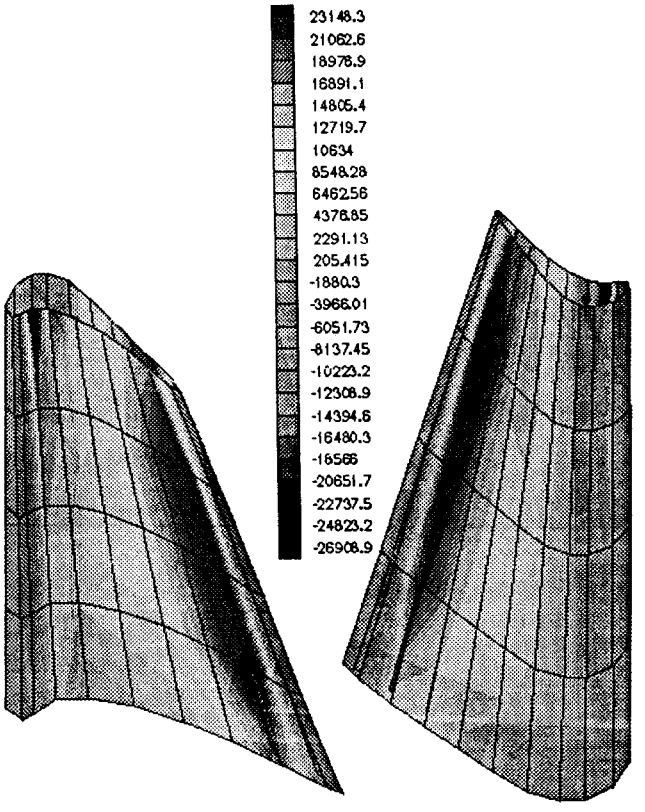

Fig. 8 Specified (desired or target) distribution of heat fluxes on the outer surface of the three-dimensional blade.

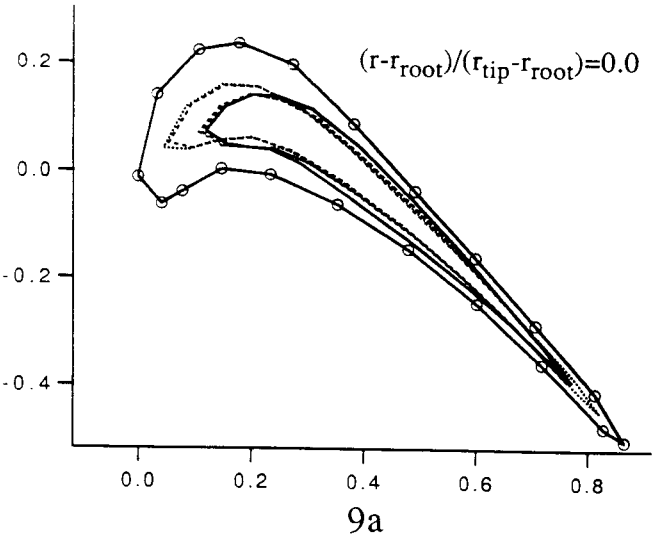

9a

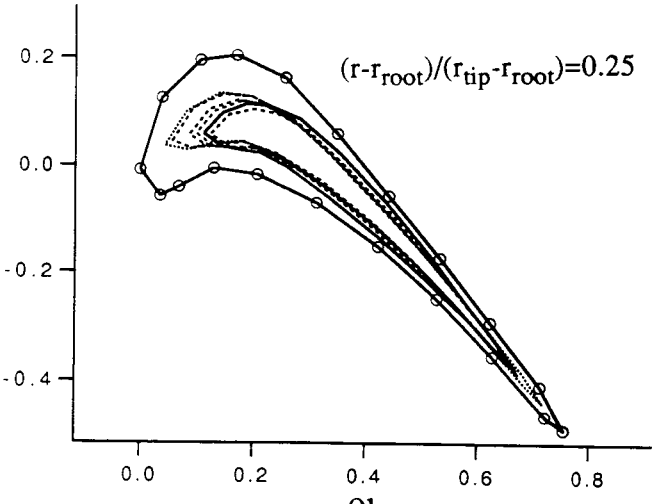

9b

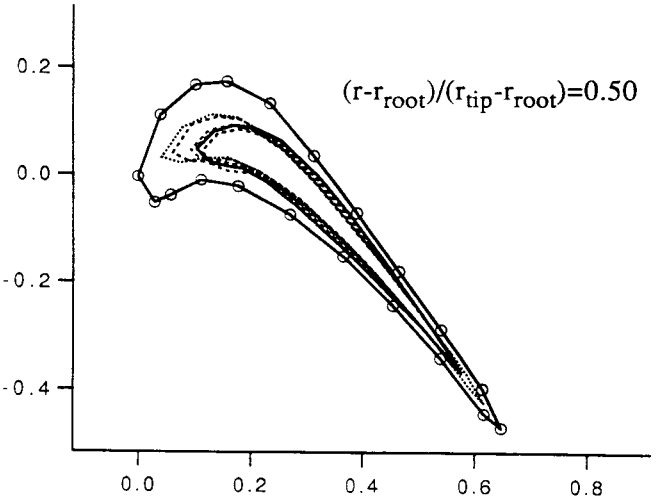

9c

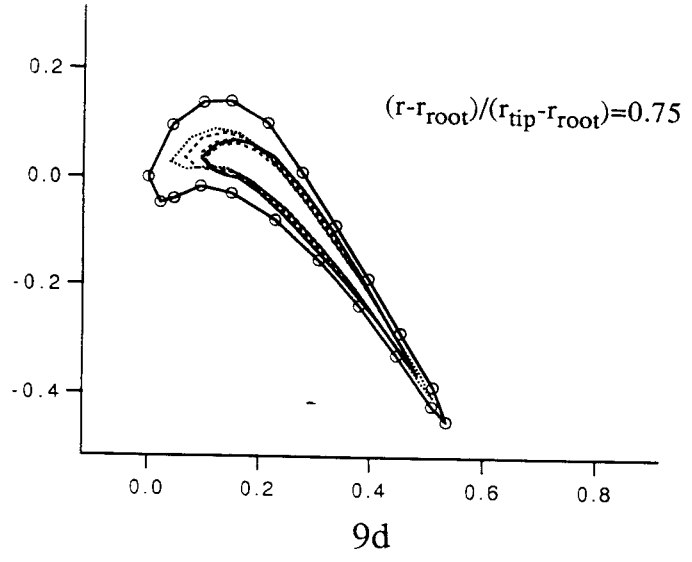

9d

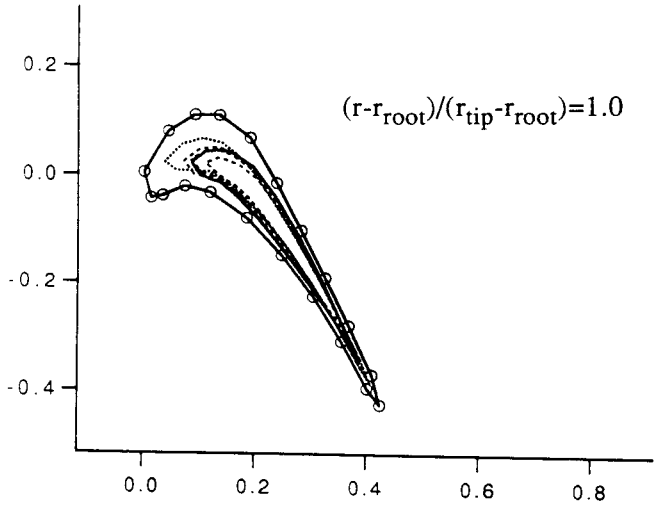

9e

Fig. 9 Geometric evolution of thickness distributions on individual cross-sections of the three-dimensional blade.

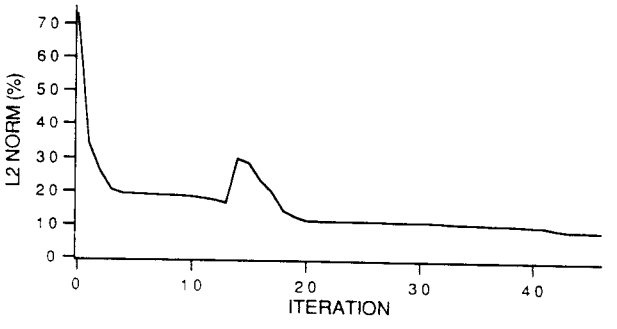

Fig. 10 Convergence history of the objective function for the three-dimensional turbine blade wall thickness optimization.